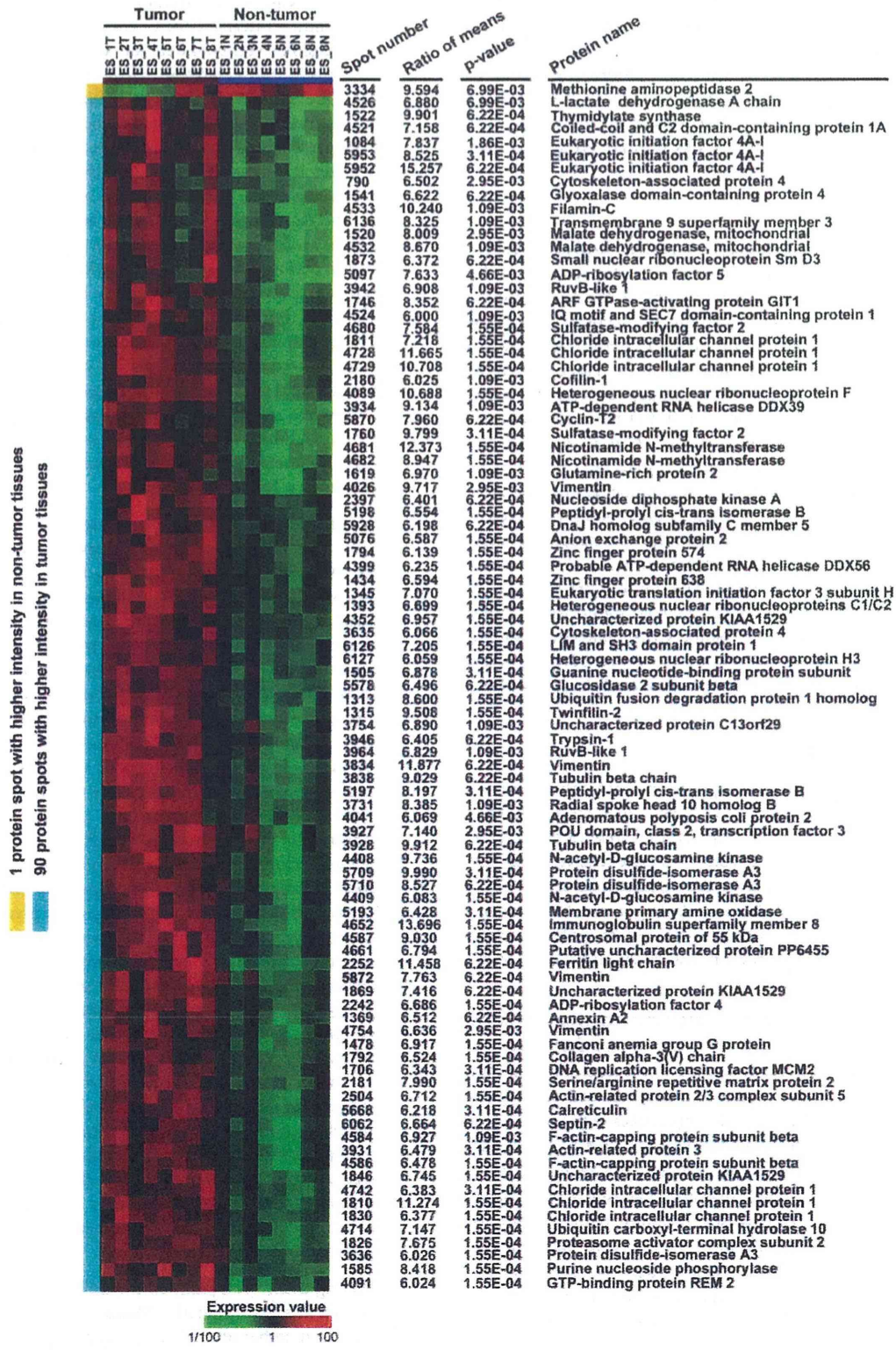


| Spot number | Ratio of means | p-value | Protein name |
|---|---|---|---|
| 3334 | 9.594 | 6.99E-03 | Methionine aminopeptidase 2 |
| 4526 | 6.880 | 6.99E-03 | L-lactate dehydrogenase A chain |
| 1522 | 9.901 | 6.22E-04 | Thymidylate synthase |
| 4521 | 7.158 | 6.22E-04 | Coiled-coil and C2 domain-containing protein 1A |
| 1084 | 7.837 | 1.86E-03 | Eukaryotic initiation factor 4A-I |
| 5953 | 8.525 | 3.11E-04 | Eukaryotic initiation factor 4A-I |
| 5952 | 15.257 | 6.22E-04 | Eukaryotic initiation factor 4A-I |
| 790 | 6.502 | 2.95E-03 | Cytoskeleton-associated protein 4 |
| 1541 | 6.622 | 6.22E-04 | Glyoxalase domain-containing protein 4 |
| 4533 | 10.240 | 1.09E-03 | Filamin-C |
| 6136 | 8.325 | 1.09E-03 | Transmembrane 9 superfamily member 3 |
| 1520 | 8.009 | 2.95E-03 | Malate dehydrogenase, mitochondrial |
| 4532 | 8.670 | 1.09E-03 | Malate dehydrogenase, mitochondrial |
| 1873 | 6.372 | 6.22E-04 | Small nuclear ribonucleoprotein Sm D3 |
| 5097 | 7.633 | 4.66E-03 | ADP-ribosylation factor 5 |
| 3942 | 6.908 | 1.09E-03 | RuvB-like 1 |
| 1746 | 8.352 | 6.22E-04 | ARF GTPase-activating protein GIT1 |
| 4524 | 6.000 | 1.09E-03 | IQ motif and SEC7 domain-containing protein 1 |
| 4680 | 7.584 | 1.55E-04 | Sulfatase-modifying factor 2 |
| 1811 | 7.218 | 1.55E-04 | Chloride intracellular channel protein 1 |
| 4728 | 11.665 | 1.55E-04 | Chloride intracellular channel protein 1 |
| 4729 | 10.708 | 1.55E-04 | Chloride intracellular channel protein 1 |
| 2180 | 6.025 | 1.09E-03 | Cofilin-1 |
| 4089 | 10.688 | 1.55E-04 | Heterogeneous nuclear ribonucleoprotein F |
| 3934 | 9.134 | 1.09E-03 | ATP-dependent RNA helicase DDX39 |
| 5870 | 7.960 | 6.22E-04 | Cyclin-T2 |
| 1760 | 9.799 | 3.11E-04 | Sulfatase-modifying factor 2 |
| 4681 | 12.373 | 1.55E-04 | Nicotinamide N-methyltransferase |
| 4682 | 8.947 | 1.55E-04 | Nicotinamide N-methyltransferase |
| 1619 | 6.970 | 1.09E-03 | Glutamine-rich protein 2 |
| 4026 | 9.717 | 2.95E-03 | Vimentin |
| 2397 | 6.401 | 6.22E-04 | Nucleoside diphosphate kinase A |
| 5198 | 6.554 | 1.55E-04 | Peptidyl-prolyl cis-trans isomerase B |
| 5928 | 6.198 | 6.22E-04 | DnaJ homolog subfamily C member 5 |
| 5076 | 6.587 | 1.55E-04 | Anion exchange protein 2 |
| 1794 | 6.139 | 1.55E-04 | Zinc finger protein 574 |
| 4399 | 6.235 | 1.55E-04 | Probable ATP-dependent RNA helicase DDX56 |
| 1434 | 6.594 | 1.55E-04 | Zinc finger protein 638 |
| 1345 | 7.070 | 1.55E-04 | Eukaryotic translation initiation factor 3 subunit H |
| 1393 | 6.699 | 1.55E-04 | Heterogeneous nuclear ribonucleoproteins C1/C2 |
| 4352 | 6.957 | 1.55E-04 | Uncharacterized protein KIAA1529 |
| 3635 | 6.066 | 1.55E-04 | Cytoskeleton-associated protein 4 |
| 6126 | 7.205 | 1.55E-04 | LIM and SH3 domain protein 1 |
| 6127 | 6.059 | 1.55E-04 | Heterogeneous nuclear ribonucleoprotein H3 |
| 1505 | 6.878 | 3.11E-04 | Guanine nucleotide-binding protein subunit |
| 5578 | 6.496 | 6.22E-04 | Glucosidase 2 subunit beta |
| 1313 | 8.600 | 1.55E-04 | Ubiquitin fusion degradation protein 1 homolog |
| 1315 | 9.508 | 1.55E-04 | Twinfilin-2 |
| 3754 | 6.890 | 1.09E-03 | Uncharacterized protein C13orf29 |
| 3946 | 6.405 | 6.22E-04 | Trypsin-1 |
| 3964 | 6.829 | 1.09E-03 | RuvB-like 1 |
| 3834 | 11.877 | 6.22E-04 | Vimentin |
| 3838 | 9.029 | 6.22E-04 | Tubulin beta chain |
| 5197 | 8.197 | 3.11E-04 | Peptidyl-prolyl cis-trans isomerase B |
| 3731 | 8.385 | 1.09E-03 | Radial spoke head 10 homolog B |
| 4041 | 6.069 | 4.66E-03 | Adenomatous polyposis coli protein 2 |
| 3927 | 7.140 | 2.95E-03 | POU domain, class 2, transcription factor 3 |
| 3928 | 9.912 | 6.22E-04 | Tubulin beta chain |
| 4408 | 9.736 | 1.55E-04 | N-acetyl-D-glucosamine kinase |
| 5709 | 9.990 | 3.11E-04 | Protein disulfide-isomerase A3 |
| 5710 | 8.527 | 6.22E-04 | Protein disulfide-isomerase A3 |
| 4409 | 6.083 | 1.55E-04 | N-acetyl-D-glucosamine kinase |
| 5193 | 6.428 | 3.11E-04 | Membrane primary amine oxidase |
| 4652 | 13.696 | 1.55E-04 | Immunoglobulin superfamily member 8 |
| 4587 | 9.030 | 1.55E-04 | Centrosomal protein of 55 kDa |
| 4661 | 6.794 | 1.55E-04 | Putative uncharacterized protein PP6455 |
| 2252 | 11.458 | 6.22E-04 | Ferritin light chain |
| 5872 | 7.763 | 6.22E-04 | Vimentin |
| 1869 | 7.416 | 6.22E-04 | Uncharacterized protein KIAA1529 |
| 2242 | 6.686 | 1.55E-04 | ADP-ribosylation factor 4 |
| 1369 | 6.512 | 6.22E-04 | Annexin A2 |
| 4754 | 6.636 | 2.95E-03 | Vimentin |
| 1478 | 6.917 | 1.55E-04 | Fanconi anemia group G protein |
| 1792 | 6.524 | 1.55E-04 | Collagen alpha-3(V) chain |
| 1706 | 6.343 | 3.11E-04 | DNA replication licensing factor MCM2 |
| 2181 | 7.990 | 1.55E-04 | Serine/arginine repetitive matrix protein 2 |
| 2504 | 6.712 | 1.55E-04 | Actin-related protein 2/3 complex subunit 5 |
| 5668 | 6.218 | 3.11E-04 | Calreticulin |
| 6062 | 6.664 | 6.22E-04 | Septin-2 |
| 4584 | 6.927 | 1.09E-03 | F-actin-capping protein subunit beta |
| 3931 | 6.479 | 3.11E-04 | Actin-related protein 3 |
| 4586 | 6.478 | 1.55E-04 | F-actin-capping protein subunit beta |
| 1846 | 6.745 | 1.55E-04 | Uncharacterized protein KIAA1529 |
| 4742 | 6.383 | 3.11E-04 | Chloride intracellular channel protein 1 |
| 1810 | 11.274 | 1.55E-04 | Chloride intracellular channel protein 1 |
| 1830 | 6.377 | 1.55E-04 | Chloride intracellular channel protein 1 |
| 4714 | 7.147 | 1.55E-04 | Ubiquitin carboxyl-terminal hydrolase 10 |
| 1826 | 7.675 | 1.55E-04 | Proteasome activator complex subunit 2 |
| 3636 | 6.026 | 1.55E-04 | Protein disulfide-isomerase A3 |
| 1585 | 8.418 | 1.55E-04 | Purine nucleoside phosphorylase |
| 4091 | 6.024 | 1.55E-04 | GTP-binding protein REM 2 |

**Figure 2:** Results of comparative 2D-DIGE and protein identification by mass spectrometry. The results of the protein expression study are summarized in the form of a heat map. The results of protein identification are shown on the left side of the heat map. The protein spot numbers correspond to those in Figure 1B and Table 2.

| Spot no.[a] | Accession no.[b] | Symbol | Identified protein | P value | Fold difference | pI[c] (obs) | MW[c] (obs)(Da) | Protein score[d] | Peptide matches | Peptide sequence coverage (%) |
|---|---|---|---|---|---|---|---|---|---|---|
| 790 | Q07065 | CKAP4 | Cytoskeleton-associated protein 4 | 2.95E-03 | 6.502 | 5.63 | 66097 | 1007 | 21 | 38 |
| 1084 | B4E102 | IF4A1 | Eukaryotic initiation factor 4A-I | 1.86E-03 | 7.837 | 5.32 | 46353 | 68 | 1 | 2.5 |
| 1313 | Q92890 | UFD1 | Ubiquitin fusion degradation protein 1 homolog | 1.55E-04 | 8.600 | 6.27 | 34763 | 59 | 1 | 4.9 |
| 1315 | Q6IBS0 | TWF2 | Twinfilin-2 | 1.55E-04 | 9.508 | 6.37 | 39751 | 593 | 13 | 36.1 |
| 1345 | O15372 | EIF3H | Eukaryotic translation initiation factor 3 subunit H | 1.55E-04 | 7.070 | 6.09 | 40076 | 102 | 2 | 5.4 |
| 1369 | P07355 | ANXA2 | Annexin A2 | 6.22E-04 | 6.512 | 7.57 | 38808 | 316 | 6 | 18.3 |
| 1393 | P07910 | HNRPC | Heterogeneous nuclear ribonucleoproteins C1/C2 | 1.55E-04 | 6.699 | 4.95 | 33707 | 192 | 5 | 15.4 |
| 1434 | Q14966 | ZN638 | Zinc finger protein 638 | 1.55E-04 | 6.594 | 6.02 | 221914 | 48 | 1 | 1.2 |
| 1478 | O15287 | FANCG | Fanconi anemia group G protein | 1.55E-04 | 6.917 | 5.32 | 69423 | 45 | 1 | 2.7 |
| 1505 | G3V2C9 | GBLP | Guanine nucleotide-binding protein subunit beta-2-like 1 | 3.11E-04 | 6.878 | 7.6 | 35511 | 508 | 8 | 30 |
| 1520 | P40926 | MDHM | Malate dehydrogenase, mitochondrial | 2.95E-03 | 8.009 | 8.92 | 35937 | 48 | 1 | 3.3 |
| 1522 | P04818 | TYSY | Thymidylate synthase | 6.22E-04 | 9.901 | 6.51 | 35978 | 440 | 9 | 28.1 |
| 1541 | Q9HC38 | GLOD4 | Glyoxalase domain-containing protein 4 | 6.22E-04 | 6.622 | 5.4 | 35170 | 51 | 1 | 4.2 |
| 1585 | P00491 | PNPH | Purine nucleoside phosphorylase | 1.55E-04 | 8.418 | 6.45 | 32325 | 784 | 20 | 55.4 |
| 1619 | Q9H0J4 | QRIC2 | Glutamine-rich protein 2 | 1.09E-03 | 6.970 | 6.25 | 181228 | 40 | 1 | 0.5 |
| 1706 | P49736 | MCM2 | DNA replication licensing factor MCM2 | 3.11E-04 | 6.343 | 5.34 | 102516 | 42 | 1 | 2.7 |
| 1746 | Q9Y2X7 | GIT1 | ARF GTPase-activating protein GIT1 | 6.22E-04 | 8.352 | 6.33 | 85030 | 42 | 1 | 2.1 |
| 1760 | Q8NBJ7 | SUMF2 | Sulfatase-modifying factor 2 | 3.11E-04 | 9.799 | 7.79 | 33950 | 83 | 2 | 8.6 |
| 1792 | P25940 | CO5A3 | Collagen alpha-3(V) chain | 1.55E-04 | 6.524 | 6.37 | 172631 | 40 | 1 | 0.9 |
| 1794 | Q6ZN55 | ZN574 | Zinc finger protein 574 | 1.55E-04 | 6.139 | 8.44 | 101175 | 35 | 1 | 2.1 |
| 1810 | O00299 | CLIC1 | Chloride intracellular channel protein 1 | 1.55E-04 | 11.274 | 5.09 | 27248 | 296 | 4 | 20.7 |
| 1811 | Q9HCI6 | CLIC1 | Chloride intracellular channel protein 1 | 1.55E-04 | 7.218 | 5.09 | 27248 | 276 | 4 | 20.7 |
| 1826 | Q9UL46 | PSME2 | Proteasome activator complex subunit 2 | 1.55E-04 | 7.675 | 5.44 | 27515 | 280 | 5 | 23 |
| 1830 | O00299 | CLIC1 | Chloride intracellular channel protein 1 | 1.55E-04 | 6.377 | 5.09 | 27248 | 227 | 3 | 17.4 |
| 1846 | Q9HCI6 | K1529 | Uncharacterized protein KIAA1529 | 1.55E-04 | 6.745 | 5.74 | 192404 | 48 | 2 | 1.2 |
| 1869 | Q9HCI7 | K1529 | Uncharacterized protein KIAA1529 | 6.22E-04 | 7.416 | 5.74 | 192404 | 46 | 4 | 1.2 |
| 1873 | P62318 | SMD3 | Small nuclear ribonucleoprotein Sm D3 | 6.22E-04 | 6.372 | 10.33 | 14021 | 35 | 1 | 8.7 |
| 2180 | P23528 | COF1 | Cofilin-1 | 1.09E-03 | 6.025 | 8.22 | 18719 | 293 | 4 | 37.3 |
| 2181 | Q9UQ35 | SRRM2 | Serine/arginine repetitive matrix protein 2 | 1.55E-04 | 7.990 | 12.05 | 300179 | 36 | 1 | 1.1 |
| 2242 | P18085 | ARF4 | ADP-ribosylation factor 4 | 1.55E-04 | 6.686 | 6.59 | 20612 | 168 | 3 | 15.6 |
| 2252 | P02792 | FRIL | Ferritin light chain | 6.22E-04 | 11.458 | 5.51 | 20064 | 125 | 2 | 17.1 |
| 2397 | C9K028 | NDKA | Nucleoside diphosphate kinase A | 6.22E-04 | 6.401 | 5.83 | 17309 | 447 | 13 | 64.5 |
| 2504 | O15511 | ARPC5 | Actin-related protein 2/3 complex subunit 5 | 1.55E-04 | 6.712 | 5.47 | 16367 | 293 | 7 | 29.1 |
| 3334 | P50579 | AMPM2 | Methionine aminopeptidase 2 | 6.99E-03 | 9.594 | 5.57 | 53713 | 36 | 1 | 3.6 |
| 3635 | Q07065 | CKAP4 | Cytoskeleton-associated protein 4 | 1.55E-04 | 6.066 | 5.63 | 66097 | 1209 | 18 | 38.7 |
| 3636 | P30101 | PDIA3 | Protein disulfide-isomerase A3 | 1.55E-04 | 6.026 | 5.98 | 57146 | 1312 | 25 | 46.1 |
| 3731 | P0C881 | R10B1 | Radial spoke head 10 homolog B | 1.09E-03 | 8.385 | 7.16 | 101255 | 35 | 1 | 2 |
| 3754 | Q8IVM7 | CM029 | Uncharacterized protein C13orf29 | 1.09E-03 | 6.890 | 9.29 | 18425 | 39 | 1 | 11 |
| 3834 | P08670 | VIME | Vimentin | 6.22E-04 | 11.877 | 5.06 | 53676 | 1794 | 41 | 60.3 |
| 3838 | E9PBJ4 | TBB5 | Tubulin beta chain | 6.22E-04 | 9.029 | 4.78 | 50095 | 301 | 8 | 13.7 |
| 3927 | Q9VKI9 | PO2F3 | POU domain, class 2, transcription factor 3 | 2.95E-03 | 7.140 | 8.81 | 47764 | 36 | 1 | 3.9 |
| 3928 | E9PBJ4 | TBB5 | Tubulin beta chain | 6.22E-04 | 9.912 | 4.78 | 50095 | 310 | 7 | 15.3 |
| 3931 | P61158 | ARP3 | Actin-related protein 3 | 3.11E-04 | 6.479 | 5.61 | 47797 | 618 | 12 | 25.6 |
| 3934 | O00148 | DDX39 | ATP-dependent RNA helicase DDX39 | 1.09E-03 | 9.134 | 5.46 | 49611 | 533 | 10 | 25.1 |
| 3942 | Q9Y265 | RUVB1 | RuvB-like 1 | 1.09E-03 | 6.908 | 6.02 | 50538 | 175 | 4 | 8.6 |
| 3946 | E7EQ64 | TRY1 | Trypsin-1 | 6.22E-04 | 6.405 | 6.08 | 27111 | 46 | 1 | 4 |
| 3964 | Q9Y265 | RUVB1 | RuvB-like 1 | 1.09E-03 | 6.829 | 6.02 | 50538 | 984 | 17 | 37.3 |
| 4026 | P08670 | VIME | Vimentin | 2.95E-03 | 9.717 | 5.06 | 53676 | 167 | 3 | 7.9 |
| 4041 | O95996 | APC2 | Adenomatous polyposis coli protein 2 | 4.66E-03 | 6.069 | 9.08 | 245966 | 36 | 1 | 0.6 |
| 4089 | P52597 | HNRPF | Heterogeneous nuclear ribonucleoprotein F | 1.55E-04 | 10.688 | 5.38 | 45985 | 146 | 2 | 8 |
| 4091 | Q8IYK8 | REM2 | GTP-binding protein REM 2 | 1.55E-04 | 6.024 | 9.19 | 36170 | 38 | 1 | 8.5 |
| 4352 | B1AK85 | K1529 | Uncharacterized protein KIAA1529 | 1.55E-04 | 6.957 | 5.74 | 192404 | 44 | 3 | 1.2 |
| 4399 | Q9NY93 | DDX56 | Probable ATP-dependent RNA helicase DDX56 | 1.55E-04 | 6.235 | 9.34 | 62007 | 37 | 1 | 3.8 |
| 4408 | Q9UJ70 | NAGK | N-acetyl-D-glucosamine kinase | 1.55E-04 | 9.736 | 5.81 | 37694 | 216 | 4 | 12.8 |
| 4409 | Q9UJ70 | NAGK | N-acetyl-D-glucosamine kinase | 1.55E-04 | 6.083 | 5.81 | 37694 | 513 | 8 | 28.5 |
| 4521 | Q6P1NO | C2D1A | Coiled-coil and C2 domain-containing protein 1A | 6.22E-04 | 7.158 | 8.22 | 104397 | 51 | 1 | 1.6 |
| 4524 | Q6DN90 | IQEC1 | IQ motif and SEC7 domain-containing protein 1 | 1.09E-03 | 6.000 | 6.49 | 109103 | 34 | 1 | 1 |
| 4526 | P00338 | LDHA | L-lactate dehydrogenase A chain | 6.99E-03 | 6.880 | 8.44 | 36950 | 247 | 4 | 12 |

| | | | | | | | | | | |
|---|---|---|---|---|---|---|---|---|---|---|
| 4532 | A6NHQ2 | FBLL1 | rRNA/tRNA 2~-O-methyltransferase fibrillarin-like protein 1 | 1.09E-03 | 8.670 | 10.33 | 34711 | 41 | 1 | 3.6 |
| 4533 | Q14315 | FLNC | Filamin-C | 1.09E-03 | 10.240 | 5.68 | 293344 | 39 | 1 | 0.4 |
| 4584 | P47756 | CAPZB | F-actin-capping protein subunit beta | 1.09E-03 | 6.927 | 5.36 | 31616 | 518 | 11 | 28.2 |
| 4586 | P47756 | CAPZB | F-actin-capping protein subunit beta | 1.55E-04 | 6.478 | 5.36 | 31616 | 431 | 9 | 21.7 |
| 4587 | Q53EZ4 | CEP55 | Centrosomal protein of 55 kDa | 1.55E-04 | 9.030 | 6.52 | 54433 | 38 | 1 | 2.6 |
| 4652 | Q969P0 | IGSF8 | Immunoglobulin superfamily member 8 | 1.55E-04 | 13.696 | 8.23 | 65621 | 35 | 1 | 1.6 |
| 4661 | Q8WZ26 | YS006 | Putative uncharacterized protein PP6455 | 1.55E-04 | 6.794 | 8.26 | 15165 | 35 | 1 | 6.7 |
| 4680 | Q8NBJ7 | SUMF2 | Sulfatase-modifying factor 2 | 1.55E-04 | 7.584 | 7.79 | 33950 | 119 | 2 | 8.6 |
| 4681 | P40261 | NNMT | Nicotinamide N-methyltransferase | 1.55E-04 | 12.373 | 5.56 | 30011 | 239 | 4 | 17.4 |
| 4682 | P40261 | NNMT | Nicotinamide N-methyltransferase | 1.55E-04 | 8.947 | 5.56 | 30011 | 104 | 2 | 7.6 |
| 4714 | Q14694 | UBP10 | Ubiquitin carboxyl-terminal hydrolase 10 | 1.55E-04 | 7.147 | 5.19 | 87707 | 35 | 1 | 1.9 |
| 4728 | O00299 | CLIC1 | Chloride intracellular channel protein 1 | 1.55E-04 | 11.665 | 5.09 | 27248 | 320 | 5 | 24.1 |
| 4729 | O00299 | CLIC1 | Chloride intracellular channel protein 1 | 1.55E-04 | 10.708 | 5.09 | 27248 | 176 | 3 | 17.4 |
| 4742 | O00299 | CLIC1 | Chloride intracellular channel protein 1 | 3.11E-04 | 6.383 | 5.09 | 27248 | 60 | 1 | 5 |
| 4754 | P08670 | VIME | Vimentin | 2.95E-03 | 6.636 | 5.06 | 53676 | 212 | 4 | 10.5 |
| 5076 | C9J035 | B3A2 | Anion exchange protein 2 | 1.55E-04 | 6.587 | 5.9 | 137493 | 41 | 1 | 1 |
| 5097 | P84085 | ARF5 | ADP-ribosylation factor 5 | 4.66E-03 | 7.633 | 6.3 | 20631 | 278 | 5 | 34.4 |
| 5193 | Q16853 | AOC3 | Membrane primary amine oxidase | 3.11E-04 | 6.428 | 6.05 | 85138 | 37 | 1 | 2.5 |
| 5197 | P23284 | PPIB | Peptidyl-prolyl cis-trans isomerase B | 3.11E-04 | 8.197 | 9.42 | 23785 | 427 | 11 | 34.7 |
| 5198 | P23284 | PPIB | Peptidyl-prolyl cis-trans isomerase B | 1.55E-04 | 6.554 | 9.42 | 23785 | 202 | 5 | 23.6 |
| 5578 | P14314 | GLU2B | Glucosidase 2 subunit beta | 6.22E-04 | 6.496 | 4.33 | 60357 | 205 | 3 | 8.1 |
| 5668 | P27797 | CALR | Calreticulin | 3.11E-04 | 6.218 | 4.29 | 48283 | 213 | 5 | 8.6 |
| 5709 | P30101 | PDIA3 | Protein disulfide-isomerase A3 | 3.11E-04 | 9.990 | 5.98 | 57146 | 565 | 12 | 22.8 |
| 5710 | P30101 | PDIA3 | Protein disulfide-isomerase A3 | 6.22E-04 | 8.527 | 5.98 | 57146 | 696 | 12 | 26.1 |
| 5870 | O60583 | CCNT2 | Cyclin-T2 | 6.22E-04 | 7.960 | 9.04 | 81492 | 39 | 1 | 1.6 |
| 5872 | P08670 | VIME | Vimentin | 6.22E-04 | 7.763 | 5.06 | 53676 | 952 | 22 | 37.1 |
| 5928 | Q9H3Z4 | DNJC5 | DnaJ homolog subfamily C member 5 | 6.22E-04 | 6.198 | 4.93 | 22933 | 43 | 1 | 10.1 |
| 5952 | Q07065 | IF4A1 | Eukaryotic initiation factor 4A-I | 6.22E-04 | 15.257 | | 46353 | | 1 | 2.5 |
| 5953 | Q07065 | IF4A1 | Eukaryotic initiation factor 4A-I | 3.11E-04 | 8.525 | | 46353 | | 10 | 23.4 |
| 6062 | Q15019 | SEPT | Septin-2 | 6.22E-04 | 6.664 | | 41689 | | 3 | 8.6 |
| 6126 | Q14847 | LASP1 | LIM and SH3 domain protein 1 | 1.55E-04 | 7.205 | | 30097 | | 3 | 15.3 |
| 6127 | B4DHY1 | HNRH3 | Heterogeneous nuclear ribonucleoprotein H3 | 1.55E-04 | 6.059 | | 36960 | | 1 | 3.5 |
| 6136 | Q5TB53 | TM9S3 | Transmembrane 9 superfamily member 3 | 1.09E-03 | 8.325 | | 68584 | | 1 | 2 |

[a]Spot numbers refer to those in Figure 1B.
[b]Accession numbers of proteins were derived from Swiss-Plot and NBCI nonredundant data bases.
[c]Observed isoelectric point and molecular weight calculated according to location on the 2D gel.
[d]Mascot score for the identified proteins based on the peptide ions score ($p < 0.05$) (http://www.matrixscience.com).

**Table 2:** A list of identified proteins with differential expression between tumor and non-tumor tissues in ES patients.

been investigated. The family protein of CAPZB was implemented in the other types of cancers. For instance, using a proteomics approach, we previously found that macrophage-capping protein (CapG), an actin-capping protein that blocks the barbed ends of F-actin filaments, was associated with resistance of cholangiocellular carcinoma (CCC) to gemcitabine therapy, and using immunohistochemistry we also found that CapG in tumor cells had prognostic utility [23]. Using a proteomics approach, we also found that CapG in tumor tissues was significantly associated with malignant features of gastric cancer [24]. In liver cancer, we reported that CapG was highly expressed in primary tumor tissues with intravascular metastasis [25], and the expression of CapG was confirmed in tumor cells by immnuhositochemistry and the functional significances of CapG in liver cancer cells were confirmed by *in vitro* experiments. In breast cancer, higher expression of CapG was observed at the tumor margin, suggesting that that CapG may be involved in tumor cell dissemination and metastasis [26]. These observations suggest that CapG may have diagnostic utility. Recently, van Impe et al. [27] developed a novel nanobody, which is a single-domain antibody, against CapG, and delivered it to breast cancer cells by lentiviral transduction. This resulted in attenuation of cell migration and lung metastasis, and suggested that CapG may have utility as a therapeutic target. As CAPZB has a function similar to that of CapG in actin organization, we further investigated the expression of CAPZB in tumor tissues of ES.

We confirmed overexpression of CAPZB in ES using Western blotting (Figure 3A). In all eight ES cases, we found that CAPZB was highly expressed in tumor tissues relative to adjacent non-tumor tissues ($p<0.01$, Figure 3B). These observations were consistent with those of 2D-DIGE, and mass spectrometry supported the correct identification of the protein.

We tried to localize the expression of CAPZB in specific cell types by immunohistochemistry. The immunohistochemical examination is critical in the proteomic study of ES when the tissues are homogenized for protein extraction. The tumor tissues of ES are highly complex, and the proteomic data of the homogenized tissue samples should consist of the mixed proteome data of different cell types. The laser microdissection was often employed to approach the tissue complexity. However, as the conventional laser microdissection for 2D-DIGE does not recover individual single cells [14], it cannot solve the problem of high tissue complexity of ES. To determine the expression of given proteins in tumor cells, immunohistochemistry is mandatory. Without localization data, the further in vitro functional studies cannot be significant. We stained the sectioned tissues with the antibody

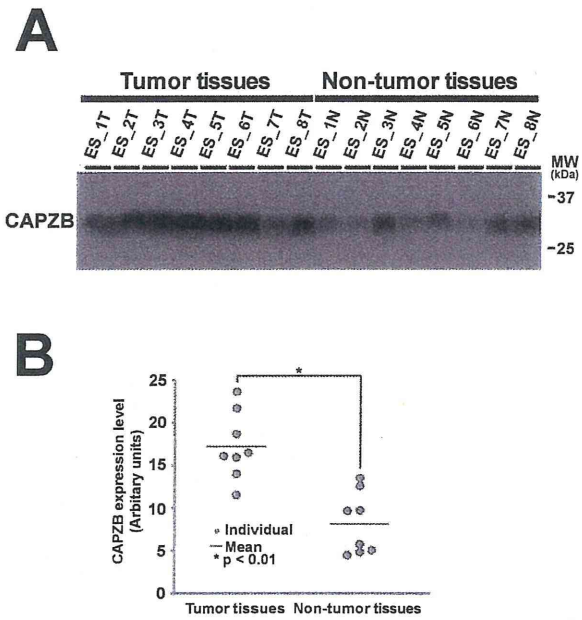


**Figure 3:** Validation study of the expression of CAPZB in tumor and non-tumor tissues. Western blotting shows that CAPZB was highly expressed in tumor tissues, relative to adjacent non-tumor tissues (A). Quantified data from Western blotting show that CAPZB expression was significantly higher in tumor tissues than in non-tumor tissues ($p<0.01$) (B).

against CAPZB, which was used for Western blotting. We found that the immunohistochemical staining patterns of CAPZB was not conclusive; the immnuhistochemical signals of CAPZB seemed to be non specific and the cellular localization of CAPZB were not consistent among the tissue sections. It may be reasoned by the characters of antibody used in this study; the indication of CAPZB antibody for immunohistochemistry was not guaranteed by antibody supplier. Presently, we could not concluded the cell types where CAPZB localized in tumor tissues of ES. It is worth screening the antibodies which can clearly localize CAPZB in tumor tissues.

Our present study has demonstrated that a proteomics approach can generate intriguing results using tissue samples. At the same time, our study clearly indicated the difficult part of tissue proteomics. Tumor tissues generally contain multiple types of cells, and localization of proteins identified by tissue proteomics should be determined prior to further examinations. However, laser microdissection may not always be a solution for tissue complexity, and immnuhistochemical examination to localize the identified proteins does not always work as expected. This inherent drawback of tissue proteomics should be considered when we interpret the proteome data of ES in this study.

## Acknowledgements

This work was supported by the National Cancer Center Research Core Facility and the National Cancer Center Research and Development Fund (23-A-7, 23-A-10, and 26-A-9). We appreciate an excellent technical support by Yukiko Nakamura (National Cancer Center Research Institute).

## References

1. Enzinger FM (1970) Epitheloid sarcoma. A sarcoma simulating a granuloma or a carcinoma. Cancer 26: 1029-1041.
2. Chase DR, Enzinger FM (1985) Epithelioid sarcoma. Diagnosis, prognostic indicators, and treatment. Am J Surg Pathol 9: 241-263.
3. Guillou L, Wadden C, Coindre JM, Krausz T, Fletcher CD (1997) "Proximal-type" epithelioid sarcoma, a distinctive aggressive neoplasm showing rhabdoid features. Clinicopathologic, immunohistochemical, and ultrastructural study of a series. Am J Surg Pathol 21: 130-146.
4. Chbani L, Guillou L, Terrier P, Decouvelaere AV, Grégoire F, et al. (2009) Epithelioid sarcoma: a clinicopathologic and immunohistochemical analysis of 106 cases from the French sarcoma group. Am J Clin Pathol 131: 222-227.
5. Fisher C (2006) Epithelioid sarcoma of Enzinger. Adv Anat Pathol 13: 114-121.
6. Evans HL, Baer SC (1993) Epithelioid sarcoma: a clinicopathologic and prognostic study of 26 cases. Semin Diagn Pathol 10: 286-291.
7. Baratti D, Pennacchioli E, Casali PG, Bertulli R, Lozza L, et al. (2007) Epithelioid sarcoma: prognostic factors and survival in a series of patients treated at a single institution. Ann Surg Oncol 14: 3542-3551.
8. Modena P, Lualdi E, Facchinetti F, Galli L, Teixeira MR, et al. (2005) SMARCB1/INI1 tumor suppressor gene is frequently inactivated in epithelioid sarcomas. Cancer Res 65: 4012-4019.
9. Hornick JL, Dal Cin P, Fletcher CD (2009) Loss of INI1 expression is characteristic of both conventional and proximal-type epithelioid sarcoma. Am J Surg Pathol 33: 542-550.
10. Brenca M, Rossi S, Lorenzetto E, Piccinin E, Piccinin S, et al. (2013) SMARCB1/INI1 genetic inactivation is responsible for tumorigenic properties of epithelioid sarcoma cell line VAESBJ. Mol Cancer Ther 12: 1060-1072.
11. Papp G, Krausz T, Stricker TP, Szendroi M, Sapi Z (2014) SMARCB1 expression in epithelioid sarcoma is regulated by miR-206, miR-38, and miR-671-5p on Both mRNA and protein levels. Genes Chromosomes Cancer 53: 168-176.
12. Weber A, Engers R, Nockemann S, Gohr LL, Zur Hausen A, et al. (2001) Differentially expressed genes in association with in vitro invasiveness of human epithelioid sarcoma. Mol Pathol 54: 324-330.
13. Lushnikova T, Knuutila S, Miettinen M (2000) DNA copy number changes in epithelioid sarcoma and its variants: a comparative genomic hybridization study. Mod Pathol 13: 1092-1096.
14. Kondo T, Hirohashi S (2007) Application of highly sensitive fluorescent dyes (CyDye DIGE Fluor saturation dyes) to laser microdissection and two-dimensional difference gel electrophoresis (2D-DIGE) for cancer proteomics. Nat Protoc 1: 2940-2956.
15. Unlü M, Morgan ME, Minden JS (1997) Difference gel electrophoresis: a single gel method for detecting changes in protein extracts. Electrophoresis 18: 2071-2077.
16. Shaw J, Rowlinson R, Nickson J, Stone T, Sweet A, et al. (2003) Evaluation of saturation labelling two-dimensional difference gel electrophoresis fluorescent dyes. Proteomics 3: 1181-1195.
17. Righetti PG (1990) Immobilized pH gradients: theory and methodology, Elsevier.
18. Romero-Calvo I, Ocón B, Martínez-Moya P, Suárez MD, Zarzuelo A, et al. (2010) Reversible Ponceau staining as a loading control alternative to actin in Western blots. Anal Biochem 401: 318-320.
19. Klein D, Kern RM, Sokol RZ (1995) A method for quantification and correction of proteins after transfer to immobilization membranes. Biochem Mol Biol Int 36: 59-66.
20. Barron-Casella EA, Torres MA, Scherer SW, Heng HH, Tsui LC, et al. (1995) Sequence analysis and chromosomal localization of human Cap Z. Conserved residues within the actin-binding domain may link Cap Z to gelsolin/severin and profilin protein families. J Biol Chem 270: 21472-21479.
21. Bai SW, Herrera-Abreu MT, Rohn JL, Racine V, Tajadura V, et al. (2011) Identification and characterization of a set of conserved and new regulators of cytoskeletal organization, cell morphology and migration. BMC Biol 9: 54.
22. Kamo M, Sato N (2006) Proteins profiling of human salivary intercalated duct cell line by proteomics. Japanese Journal of Tissue Culture Dental Research 15: 11-28.
23. Morofuji N, Ojima H, Onaya H, Okusaka T, Shimada K, et al. (2012) Macrophage-capping protein as a tissue biomarker for prediction of response to gemcitabine treatment and prognosis in cholangiocarcinoma. J Proteomics 75: 1577-1589.
24. Ichikawa H, Kanda T, Kosugi S, Kawachi Y, Sasaki H, et al. (2013) Laser

microdissection and two-dimensional difference gel electrophoresis reveal the role of a novel macrophage-capping protein in lymph node metastasis in gastric cancer. J Proteome Res 12: 3780-3791.

25. Kimura K, Ojima H, Kubota D, Sakumoto M, Nakamura Y, et al. (2013) Proteomic identification of the macrophage-capping protein as a protein contributing to the malignant features of hepatocellular carcinoma. J Proteomics 78: 362-373.

26. Kang S, Kim MJ, An H, Kim BG, Choi YP, et al. (2010) Proteomic molecular portrait of interface zone in breast cancer. J Proteome Res 9: 5638-5645.

27. Van Impe K, Bethuyne J, Cool S, Impens F, Ruano-Gallego D, et al. (2013) A nanobody targeting the F-actin capping protein CapG restrains breast cancer metastasis. Breast Cancer Res 15: R116.

**Citation:** Mukaihara K, Kubota D, Yoshida A, Asano N, Suehara Y, et al. (2014) Proteomic Profile of Epithelioid Sarcoma. J Proteomics Bioinform 7: 158-165. doi:10.4172/jpb.1000316

nature COMMUNICATIONS

ARTICLE

Received 11 Feb 2014 | Accepted 6 Mar 2014 | Published 7 Apr 2014

DOI: 10.1038/ncomms4591 OPEN

# Ultra-sensitive liquid biopsy of circulating extracellular vesicles using ExoScreen

Yusuke Yoshioka[1,2,3], Nobuyoshi Kosaka[1], Yuki Konishi[1,4], Hideki Ohta[5], Hiroyuki Okamoto[5], Hikaru Sonoda[5], Ryoji Nonaka[6], Hirofumi Yamamoto[6], Hideshi Ishii[7], Masaki Mori[6], Koh Furuta[8], Takeshi Nakajima[9], Hiroshi Hayashi[4], Hajime Sugisaki[4], Hiroko Higashimoto[4], Takashi Kato[2], Fumitaka Takeshita[1] & Takahiro Ochiya[1]

Cancer cells secrete small membranous extracellular vesicles (EVs) into their microenvironment and circulation. Although their potential as cancer biomarkers has been promising, the identification and quantification of EVs in clinical samples remains challenging. Here we describe a sensitive and rapid analytical technique for profiling circulating EVs directly from blood samples of patients with colorectal cancer. EVs are captured by two types of antibodies and are detected by photosensitizer-beads, which enables us to detect cancer-derived EVs without a purification step. We also show that circulating EVs can be used for detection of colorectal cancer using the antigen CD147, which is embedded in cancer-linked EVs. This work describes a new liquid biopsy technique to sensitively detect disease-specific circulating EVs and provides perspectives in translational medicine from the standpoint of diagnosis and therapy.

[1] Division of Molecular and Cellular Medicine, National Cancer Center Research Institute, Chuo-ku, Tokyo 104-0045, Japan. [2] Integrative Bioscience and Biomedical Engineering, Graduate School of Advanced Science and Engineering, Waseda University, Shinjuku, Tokyo 162-8480, Japan. [3] Research Fellow of the Japan Society for the Promotion of Science (JSPS), Chiyoda-Ku, Tokyo 102-0083, Japan. [4] R&D Department, SRL Inc., Hino-shi, Tokyo 191-0002, Japan. [5] Diagnostics Division, Shionogi & Co., LTD., Settsu-shi, Osaka 566-0022, Japan. [6] Department of Gastroenterological Surgery, Graduated School of Medicine, Osaka University, Suita, Osaka 565-0871, Japan. [7] Department of Frontier Science for Cancer and Chemotherapy, Osaka University, Graduate School of Medicine, Suita, Osaka 565-0871, Japan. [8] Division of Clinical Laboratories, National Cancer Center Hospital, Chuo-ku Tokyo, 104-0045, Japan. [9] Endoscopy Division, National Cancer Center Hospital, Chuo-ku, Tokyo 104-0045, Japan. Correspondence and requests for materials should be addressed to T.O. (email: tochiya@ncc.go.jp).

Cancer cells secrete various types of humoral factors into their microenvironment that are biomarkers for disease diagnosis and prognosis, including cytokines, chemokines and nucleic acids. Extracellular vesicles (EVs), including exosome and microvesicles from cancer cells, have also been found in the blood of cancer patients[1–7] and therefore provide a novel type of biomarker for various patient scenarios.

EVs are small membranous vesicles that differ in their cellular origin, abundance and biogenesis[8], and are naturally secreted by almost all cell types to transport bioactive molecules intercellularly. EVs are positive for tetraspanin family proteins, such as CD63, CD81 and CD9 (refs 9–11), and contain cell surface proteins as well as both mRNA and microRNA[12]. Conventional methods of analyzing EVs generally require large quantities of EVs to be concentrated and processed via time-consuming immunoblotting or enzyme-linked immunosorbent assay (ELISA) assays; these methods are impractical in most clinical settings. In this study, we establish a highly sensitive and rapid analytical technique for profiling surface proteins in EVs from patient blood that can be used to identify biomarkers of colorectal cancer, named ExoScreen. ExoScreen could monitor circulating EVs in serum without the need for purification step. In addition, we show that ExoScreen is superior for the detection of EVs to conventional methods, immunoblotting and ELISA. Furthermore, we find that ExoScreen enables to detect CD147 and CD9 double-positive EVs, which is abundantly secreted from colorectal cancer cells, in serum from colorectal cancer patients. Our results demonstrate that ExoScreen can be a tool for detection of EVs from as little as 5 μl of cancer patients' serum to detect circulating cancer-derived EVs.

## Results

**Establishment of ExoScreen to detect EVs in serum.** To realize the usage of EVs in clinical situation, we develop methods that specifically detect circulating EVs in the serum based on an amplified luminescent proximity homogeneous assay using photosensitizer-beads[13] without a purification step of EVs

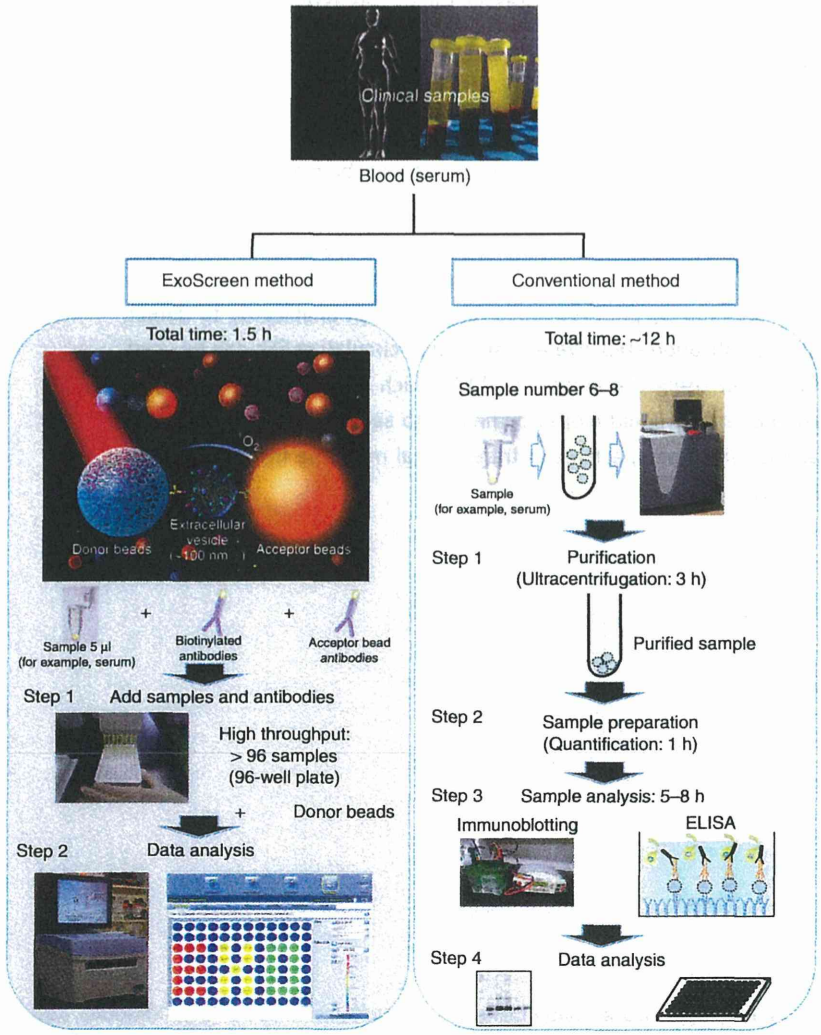


**Figure 1 | Schematic overview depicting the method for detecting circulating EVs via conventional methods and ExoScreen.** In the case of conventional methods, nearly 12 h are needed to detect the expression of certain protein in circulating EVs. In addition, excessive volumes of serum are required. Conversely, ExoScreen is completed within 2 h and requires only 5 μl of serum. In this system, streptavidin-coated donor beads capture an analyte-specific biotinylated antibody and are used in conjunction with acceptor beads conjugated to a second antibody. The streptavidin-coated donor beads are excited with a laser at 680 nm, resulting in the release of singlet oxygen, which excites an amplified fluorescent signal in the acceptor bead that emits at 615 nm when the beads are within 200 nm of the captured analyte.

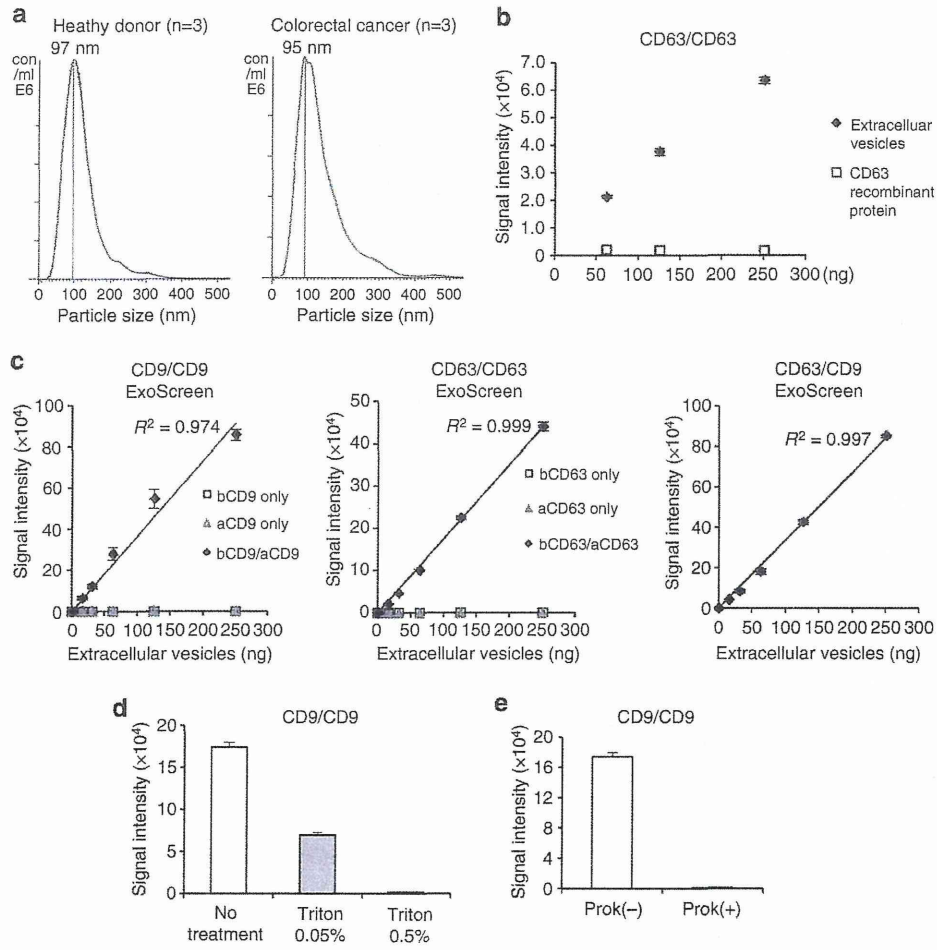


**Figure 2 | Establishment of ExoScreen to detect the EVs.** (**a**) Analysis of the size distribution in the serum of healthy donors ($n=3$) and colorectal cancer patients ($n=3$) by the NanoSight nanoparticle tracking system. (**b**) Detection of EVs or monomeric recombinant CD63 protein by ExoScreen using a CD63 antibody. EV protein concentration was measured via the Qubit system. The concentration of recombinant CD63 was adjusted with that of protein in EVs purified from HCT116 CM. Error bars are s.e.m. ($n=3$ for each condition). (**c**) Correlation between ExoScreen measurements for CD9 positive EVs, CD63 positive EVs or CD63/CD9 double-positive EVs and EV protein concentration in a dilution series. EV protein concentration was measured via the Qubit system. EVs were purified from HCT116 cell CM. The addition of biotinylated CD9 or CD63 antibodies without acceptor beads conjugated to antibodies is denoted 'bCD9 only' or 'bCD63 only', while 'aCD9 only' or 'aCD63 only' means addition of only acceptor beads conjugated to CD9 or CD63 antibodies without biotinylated antibodies. The addition of biotinylated antibodies and acceptor beads conjugated antibodies is denoted 'bCD9/aCD9' or 'bCD63/aCD63'. Right panel shows the addition of biotinylated CD63 antibodies and acceptor beads conjugated CD9 antibodies. Error bars are s.e.m. ($n=3$ for each condition). (**d**) Evaluation of ExoScreen specificity against purified EVs from HCT116 cell treated with or without 0.05% and 0.5% Triton X-100. Two hundred fifty ng of EVs were detected by ExoScreen using CD9 antibodies. Error bars are s.e.m. ($n=3$ for each condition). (**e**) Evaluation of ExoScreen specificity against EVs from HCT116 cells treated with (Prok(+)) or without (Prok(−)) Proteinase K. Two hundred fifty ng of EVs were detected by ExoScreen using CD9 antibodies. Error bars are s.e.m. ($n=3$ for each condition). Data are representative of at least three independent experiments each.

(Fig. 1). This system utilizes streptavidin-coated donor beads to capture an analyte-specific biotinylated antibody, and acceptor beads conjugated to a second antibody that recognizes an epitope of the analyte. The donor beads are excited with a laser at 680 nm, resulting in the release of singlet oxygen, which excites an amplified fluorescent signal in the acceptor beads. As a result, the acceptor beads emit light at 615 nm, but only if they are within 200 nm of the analyte captured by both antibodies. As shown in Fig. 2a, the size of EVs measured by the Nanosight particle tracking system was approximately 100 nm, which prevented the detection of larger vesicles, such as apoptotic bodies, shedding vesicles or protein complexes. In addition, we could not obtain signals from CD63 recombinant protein by ExoScreen, indicating that this assay does not detect antigen monomers (Fig. 2b). We call this assay 'ExoScreen' because the target of the assay is EVs and because it has a possibility to screen for biomarker of various diseases.

To confirm the reliability for detecting EVs by ExoScreen, we selected CD9 and CD63, which are abundant on the surface of EVs and are expressed in numerous cells, to detect EVs. Conditioned medium (CM) of prostate cancer, prostate epithelial, breast cancer and colorectal cancer cell lines were processed to obtain purified EVs. ExoScreen was able to quantify the amount of EVs present in cell culture supernatants with CD9 and CD63 positive EVs detectable in a dose-dependent manner (Fig. 2c and Supplementary Fig. 1). The negative controls, represented by only the biotinylated antibody or acceptor bead-conjugated antibody, resulted in a minimal fluorescent signal (Fig. 2c). In addition, the signal was decreased after detergent treatment (Fig. 2d and Supplementary Fig. 2) or Proteinase K treatment (Fig. 2e and

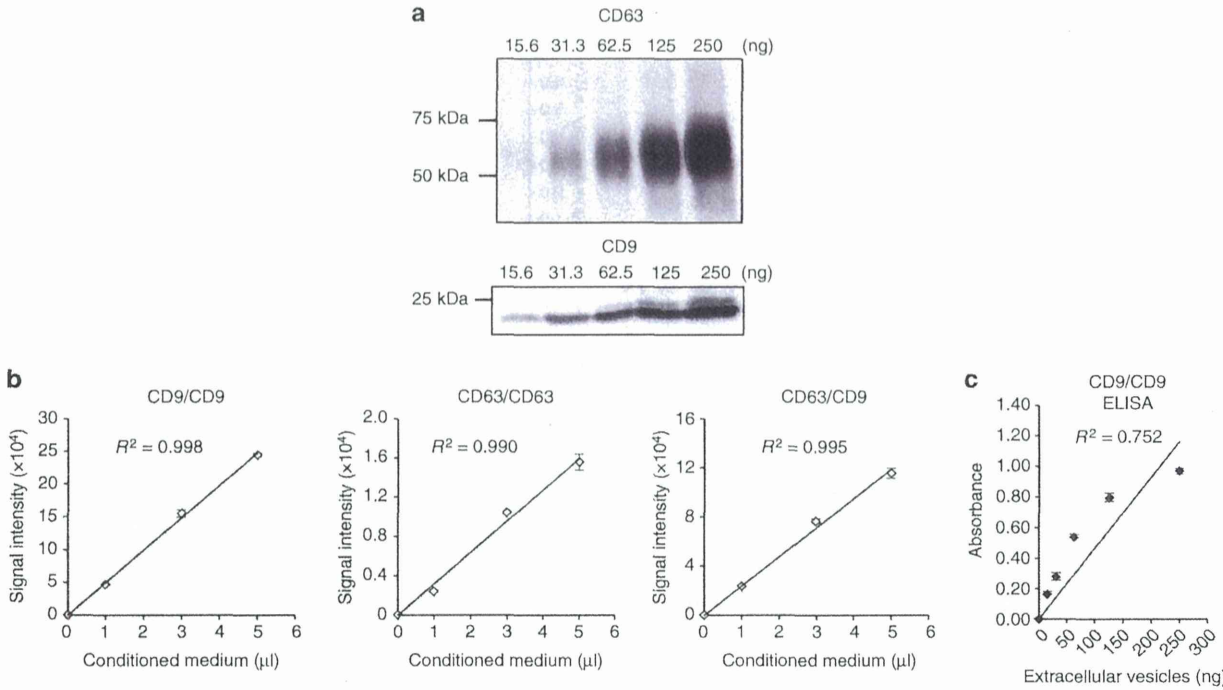


**Figure 3 | Comparison of ExoScreen and conventional methods.** (**a**) Immunoblotting analysis of CD63 (upper panels) or CD9 (lower panels) against the EVs isolated from HCT116 cells. EV protein concentration were measured via the Qubit system. EVs were purified from HCT116 cell CM. (**b**) Correlation between ExoScreen measurements for CD9 positive, CD63 positive or CD63/CD9 double-positive EVs and HCT116 cell CM in a dilution series. CM was prepared for 5 μl and diluted as indicated. Error bars are s.e.m. ($n=3$ for each condition). (**c**) Correlation between ELISA measurements for CD9 positive EVs and EV protein concentration in a dilution series. EV protein concentration were measured via the Qubit system. EVs were purified from HCT116 cell CM. Error bars are s.e.m. ($n=3$ for each condition). Data are representative of at least three independent experiments each.

**Table 1 | Comparison of ExoScreen and ELISA.**

| | ExoScreen | ELISA |
|---|---|---|
| Incubation time | 1.5–3 h | 3–6 h + coating time |
| Steps | 2 | More than 5 |
| Washes | No | Yes |
| Throughput | High | Low |
| Sample volume | Less than 5 μl* | 50–200 μl† |
| The volume of antibodies | Low | High |
| Dynamic range | 3–4 logs | 2 logs |
| Analytic range‡ | 3 orders of magnitude | 2 orders of magnitude |
| Sensitivity | High | High |
| Plate format | 96-well or 384-well | 96-well |

ELISA, enzyme-linked immunosorbent assay.
*Total assay volume 50 μl.
†Total assay volume 200 μl.
‡Calculated by CD9/CD9 analysis of EVs derived from HCT116 cells

Supplementary Fig. 3), indicating that ExoScreen detected complexes of membranous vesicle and transmembrane proteins. Immunoblotting of the same purified EVs preparations confirmed the data obtained by ExoScreen. In fact, CD9 and CD63 proteins were detectable via immunoblotting (Fig. 3a and Supplementary Fig. 4). As shown in Fig. 3a, approximately 32 ng of EV proteins were needed to properly detect CD63 by immunoblotting, while ExoScreen could detect 15.6 ng of purified EVs (Fig. 2c). Furthermore, EVs from only 1 μl of culture medium are enough to detect by ExoScreen (Fig. 3b and Supplementary Fig. 5). In addition, ExoScreen has a wide working range compared with ELISA (Figs 2c and 3c). Moreover, because ExoScreen is a mix-and-read assay, these conventional methods require many steps and substantial time compared with ExoScreen (Fig. 1). Thus, the ExoScreen assay increases throughput while substantially decreasing hands-on. Taken together, these results indicate that ExoScreen is superior for the detection of EVs to conventional immunoblotting and ELISA (Table 1). The results of EVs detection in culture supernatant without purification (Fig. 3b, Supplementary Figs 5 and 6) prompted us to investigate whether ExoScreen could detect and characterize EVs in human serum. To develop ExoScreen as a diagnostic tool for clinical use, we optimized the method to detect EVs in serum without purification because the protocol exhibited non-linearity of ExoScreen signals against serum samples (Fig. 4a). This non-linearity is most likely a result of the aggregation of condensed proteins in serum. Indeed, we added dextran-500 to suppress serum protein aggregation, and this

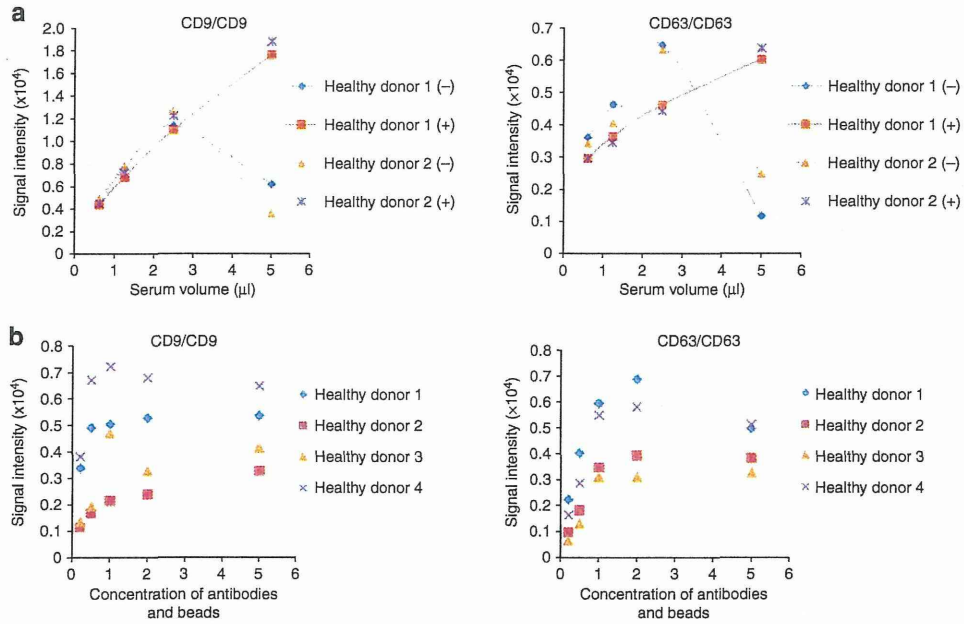


**Figure 4 | Detection of circulating EVs in healthy donor sera.** (**a**) Correlation between ExoScreen measurements for CD9 or CD63 and serum volume in a dilution series with (+) or without (−) Dextran-500. The final concentration of Dextran-500 was 1 mg ml$^{-1}$. (**b**) Concentration of '1' means the original concentration of donor and acceptor beads which we used in this study (see Methods section). In addition to original concentration, increased (twofold and fivefold) and decreased (0.5-fold and 0.25-fold) amount of donor and acceptor beads were evaluated by ExoScreen using serum from four healthy donors. Data are representative of at least three independent experiments each.

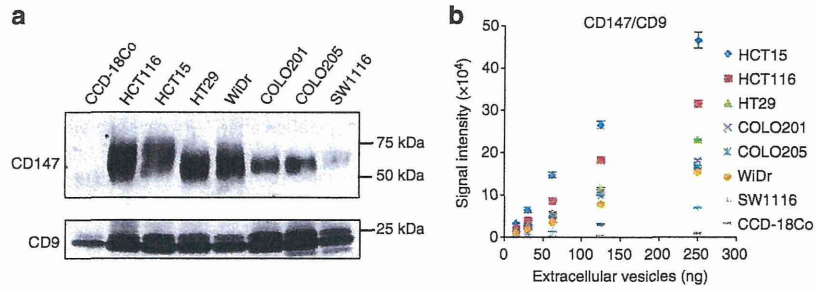


**Figure 5 | Analysis of the amount of CD147 in EVs derived from various colon cancer cell lines and a normal colon fibroblast cell line.** (**a**) Immunoblotting analysis of CD147 or CD9 against purified EVs isolated from CCD-18Co cells, HCT116 cells, HCT15 cells, HT29 cells, WiDr cells, COLO201 cells, COLO205 cells and SW1116 cells. EV proteins (250 ng) was used for the detection of CD147 and CD9. (**b**) Correlation between ExoScreen detection of CD147/CD9 double-positive EVs and EV protein concentration in a dilution series. EVs protein concentration was measured via the Qubit system. EVs were purified from CCD-18Co, HCT116, HCT15, HT29, WiDr, COLO201, COLO205 or SW1116 CM. Error bars are s.e.m. ($n=3$ for each condition). Data are representative of at least three independent experiments each.

treatment eliminated the disruption of signals by protein aggregation (Fig. 4a). As shown in Fig. 4a, ExoScreen revealed that serum EVs were captured and expressed both CD9 and CD63 without purification. Further, these signals were detectable in a dose-dependent manner (Fig. 4a). In addition, we assessed whether the concentration of beads, which we employed in this study, was appropriate for the detection of circulating EVs in serum by checking the various concentrations of beads via ExoScreen, and found that the concentration of beads we employed in this study was adequate (Fig. 4b). Taken together, these results indicated that ExoScreen could monitor circulating EVs in serum without the need for a purification process.

**Enrichment of CD147 on EVs from colorectal cancer cell lines.** Because EVs are known to represent an important and specific route of intercellular communication[14], we reasoned that tumour-derived EVs may differ from circulating EVs in normal physiological conditions. Previous reports showed that the protein components of EVs from cancer cells were different from normal cells[15,16]. Indeed, it has been recently reported that for patients with stage III melanoma, the amount of specific protein in EVs was significantly increased in individuals who eventually developed metastatic disease, indicating that EVs might have great potential for cancer diagnosis[6]. To identify cancer-derived EVs in cancer patients, EVs derived from the colorectal cancer cell line HCT116 cells and a normal colon fibroblast cell line CCD-18Co cells were subjected to proteomic analysis (Supplementary Table 1). When EVs isolated from CCD-18Co cells were compared with HCT116 cells, the amount of CD147, which is the immunoglobulin superfamily member, was found to be significantly high in the EVs of HCT116 cells, whereas the expression could not be observed in CCD-18Co cells.